and Ag(111) of 1.03 and 0.9 eV, with errors of ± 0.2 eV in these cases. I find reasonable agreement with the bulk vacancy formation enthalpies,[14] although these values are generally lower. A full derivation and discussion of the possible problems will be present elsewhere.[10]

In the recent measurements by Mills et al.,[15] where the slow-positron yield was measured as a function of temperature in Al, it was suggested that vacancy trapping was responsible for decreasing the yield of slow positrons. One should be cautious in extracting any vacancy information from these measurements as the branching ratio of Ps to free positrons may be changing at the same time, thus making the interpretation of the data very difficult or incorrect. In my measurements this effect is not significant as at the temperature at which vacancy trapping is observed, the Ps emission is close to saturation.

The present results indicate that some Ps should be emitted into voids; however, no firm evidence of Ps was found.[4] A possible explanation for these findings is that the $^3S_1$ state will cross the void and undergo spin exchange to the $^1S_0$ state. This will produce a negative result in a magnetic quenching experiment and make the bulk and surface measurements consistent.

[1]R. N. West, Adv. Phys. 22, 263 (1973). This is a general review of positrons in solids.

[2]A. Held and S. Kahana, Can. J. Phys. 42, 1908 (1964); D. N. Lowy and A. D. Jackson, Phys. Rev. B 12, 1689 (1975).

[3]K. F. Canter, A. P. Mills, Jr., and S. Berko, Phys. Rev. Lett. 33, 7 (1974).

[4]O. Mogensen, K. Petersen, R. M. J. Cotterill, and B. Hudson, Nature (London) 239, 98 (1972); R. M. J. Cotterill, I. K. Mackenzie, L. Smedskjaer, G. Trumpy, and J. H. O. L. Träff, Nature (London) 239, 99 (1972).

[5]C. H. Hodges and M. J. Stott, Solid State Commun. 18, 1115 (1976).

[6]A. P. Mills, Jr., Phys. Rev. Lett. 41, 1828 (1978).

[7]C. H. Hodges and M. J. Stott, Phys. Rev. B 7, 73 (1973).

[8]K. G. Lynn, to be published.

[9]For the 0% Ps value a difference was found between these results extrapolated to > 20 keV and the value obtained for a ^{68}Ge source sandwiched between two Ag crystals.

[10]K. G. Lynn and D. O. Welch, to be published.

[11]A. P. Mills, Jr., Bull. Am. Phys. Soc., 24, 483 (1979).

[12]The Ag(100) work function was from Handbook of Chemistry and Physics, edited by R. C. Weast (Chemical Rubber Publishing Co., Cleveland, Ohio, 1969), 49th ed.; the Cu(111) work function was obtained from P. O. Gartland and B. J. Slagsvold, Phys. Rev. B 12, 4047 (1975).

[13]R. M. Nieminen and C. H. Hodges, Phys. Rev. B 18, 2568 (1978).

[14]J. L. Campbell, C. W. Schulte, and R. R. Gingerich, J. Nucl. Mater. 69 and 70, 609 (1978).

[15]A. P. Mills, Jr., P. M. Platzman, and B. L. Brown, Phys. Rev. Lett. 41, 1076 (1978).

Picosecond Dynamics of Optically Induced Absorption in the Band Gap of As₂S₃

R. L. Fork, C. V. Shank, A. M. Glass, A. Migus,[a] M. A. Bosch, and J. Shah

Bell Telephone Laboratories, Holmdel, New Jersey 07733

(Received 1 March 1979)

Time-resolved absorption measurements are reported which imply an upper limit of 1 psec on the localization time for optically excited carriers in amorphous and crystalline As₂S₃. These measurements also imply a short recombination time in crystalline As₂S₃ ($\tau_c \approx 14$ psec), but a long recombination time in amorphous As₂S₃ ($\tau_a \gg 300$ psec). This transient induced absorption does not decrease as sharply with increasing wavelength as a previously reported metastable absorption.

Localized states in the band gap have figured prominently in phenomenological models designed to explain the transport and optical properties of amorphous semiconductors. Direct evidence for such states in the form of an optically induced metastable band-gap absorption has been reported by Bishop, Strom, and Taylor[1] for low-temperature amorphous arsenic trisulfide (a-As₂S₃). We report here an optically induced *transient* band-gap absorption in *room-temperature* a-As₂S₃ and crystalline arsenic trisulfide (c-As₂S₃) and characterize its dynamics with picosecond time reso-
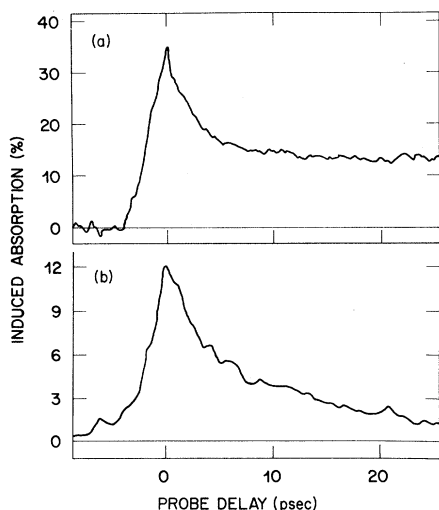
FIG. 1. Induced transient absorption vs probe delay, τ_D, for a probe at 0.63 μm, and a pump intensity of 40 GW/cm^2. For (a) amorphous, and (b) crystalline, arsenic trisulfide at 300 K.

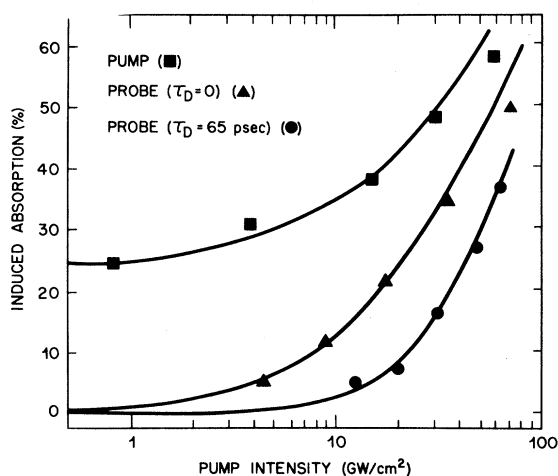FIG. 2. Induced transient absorption vs pump intensity for the pump intensity, I_p, the instantaneous probe intensity, $I_r(\tau_D = 0)$, and the delayed probe intensity, $I_r(\tau_D = 65$ psec$)$. The probe wavelength was 0.80 μm.

lution.[2,3] The close resemblance of this transient absorption to the metastable absorption observed in Ref. 1, the temporal behavior, and the agreement between the carrier mobilities implied by our observations and the previously measured mobilities[4,5] strongly suggest that this transient absorption is attributable to localized carriers. The observed dynamics thus permits deduction of the formation and relaxation times for localized carriers, and the spectra provide information concerning the distribution in energy of the occupied trapping sites at short times.

The experimental apparatus is the result of recent advances in subpicosecond pulse generation. Subpicosecond pulses (0.5 psec) from a passively mode-locked dye laser[6] operated at 0.61 μm were cavity dumped at a 10-Hz rate. These pulses were amplified to 2 GW in a dye amplifier[7] and divided into two beams. The first beam pumped the sample after passing through a variable-delay line. The second beam was focused into a cell containing H_2O or CCl_4 where it generated a broad subpicosecond continuum which, in turn, was used to probe the pump-excited sample. Filters, before the sample, and monochromators, after the sample, selected the spectral regions of interest.

The As_2S_3 glass was prepared by mixing very pure As and S (impurities < 1 ppm) in a stoichiometric ratio in a sealed silica tube. After mixing for 48 h in a rocking furnace at 600°C, the melt was quenched to room temperature in water. The

resulting glass showed no trace of impurities in the optical transmission window from 0.6 to 12 μm except for a weak absorption band ($\alpha \cong 0.5$ cm^{-1} at 10 μm) which may be attributable to oxygen. The As_2S_3 crystals were naturally occurring orpiment obtained from Nevada.

The induced absorption plotted vs probe delay, τ_D, in Fig. 1 exhibits a large absorption peak coincident with the pump pulse followed by a residual absorption with a relaxation time long compared to our resolution time of 1 psec.[8] The relaxation of the residual absorption in a-As_2S_3 could not be detected during our maximum period of observation, 300 psec; however, the residual absorption in crystalline arsenic trisulfide, c-As_2S_3, relaxed with a short time constant, 14 psec. (The induced absorption in both hosts relaxed completely, within experimental error, during the 0.1-sec interval between pulses.) The dependence of the instantaneous and residual absorptions on pump intensity was nonlinear and is shown in Fig. 2.

The temporal and nonlinear behavior observed in a-As_2S_3 can be interpreted in terms of a model in which carriers are excited by two-photon absorption,[9] and then quickly (< 1 psec) relax to long-lived states which are absorbing at the probe wavelength. The instantaneous ($\tau_D = 0$) probe absorption exhibits a peak due to a combination of two-photon absorption (one probe photon and one pump photon) and three-photon absorption (two pump photons excite a state which be-

comes absorbing in a time short compared to the pump pulse and then absorbs a probe photon). A residual absorption remains due to the long-lived absorbing states, generated primarily by absorption of two pump photons.

A reasonable approximation to the nonlinear equations relating the pump intensity, I_p, the instantaneous probe intensity, $I_r(0)$, and the delayed probe intensity, $I_r(\tau_D)$, for the above process to the one-, two-, and three-photon absorption coefficients α_0, α_1, and α_2, respectively, are

$$-I_p^{-1}\delta I_p/\delta z = \alpha_0 + \alpha_1 I_p + \tfrac{1}{2}\alpha_2 I_p^2, \tag{1}$$

$$-[I_r(0)]^{-1}\delta I_r(0)/\delta z = \alpha_1 I_p + \tfrac{1}{2}\alpha_2 I_p^2, \tag{2}$$

$$-[I_r(\tau_D)]^{-1}\delta I_r(\tau_D)\delta z = \alpha_2 I_p^2. \tag{3}$$

[We have approximated the pulse intensity and the number of induced absorbing centers as constant over the pulse duration. A phenomenological factor of $\tfrac{1}{2}$ is therefore included in the quadratic terms in (1) and (2) since the average number of centers which absorb during the pulse at $\tau_D = 0$ is half the final number of induced centers.] The calculated curves in Fig. 2 were obtained by analytically integrating Eqs. (1)–(3), and then selecting α_1 and α_2 to give the best least-squares fit. The resulting values were $\alpha_1 = 2.6\times10^{-10}$ cm/W and $\alpha_2 = 6.4\times10^{-21}$ cm^3/W^2. The linear absorption coefficient α_0 was measured to be 5.2 cm^{-1} at the pump wavelength.

The cross section σ of the induced absorbing states, and the density of induced centers N, can be determined from the relations

$$h\nu_p N = \eta\alpha_1 I_p^2\tau_p \tag{4a}$$

which relates N to the two-photon absorption [see Eq. (1)], and

$$\sigma N = \alpha_2 I_p^2 \tag{4b}$$

which relates N to the probe absorption [see Eq. (3)]. Here τ_p is the pump-pulse duration (0.5 psec, ν_p the optical frequency of the pump photons, and η the (two-photon) quantum efficiency for generation of absorbing centers. (We have also approximated the pump and probe absorption cross sections as the same. This appears justified by the flat character of the absorption spectrum.) Using the above values for α_1 and α_2 and an estimate of 0.3 for η, we find a value of σ of 10^{-16} cm^2 which is the same as that found by Bishop, Strom, and Taylor[1] for the metastable centers within experimental error.[10] We also find a value for the maximum density of induced centers of 10^{17} cm^{-3}, which is the same as that found
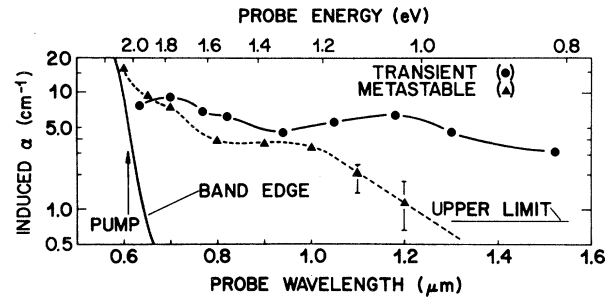

FIG. 3. Induced absorption coefficient α vs probe wavelength for a-As$_2$S$_3$. The transient absorption data were taken at 300 K for a probe delay of 15 psec and pump intensity of 50 GW/cm^2. The band edge of a-As$_2$S$_3$ and the upper limit on the metastable absorption at long wavelengths are indicated.

in Ref. 1; however, this latter agreement appears coincidental since our maximum density of transient centers was set by the need to stay below damage threshold at 10^{11} W/cm^2, rather than by evidence of saturation.

We compare the spectrum of this transient absorption with the metastable absorption induced by one-photon cw excitation at 5145 Å for temperatures $T \lesssim 80$ K in samples quenched from the same melt as the samples used for the transient absorption (Fig. 3). The observed difference we attribute to the difference between a relatively uniform distribution of occupied trapping sites[11] in the transient case and a distribution in the metastable case (as Bishop, Strom, and Taylor suggested) in which the deeply lying mid–band-gap states are selectively occupied. While this difference is suggestive of an evolution in the distribution of occupied trapping sites which eventually leads to preferential occupation of the deepest traps, an evolution for which there is independent evidence,[3,4,12] it could also be due in part to differences in excitation technique. (We also observed that our two-photon excitation technique generated metastable absorbing centers when our samples were cooled to $T < 80$ K; however, we did not map out a detailed absorption spectrum for that case.)

The temporal behavior also supports an assignment of the transient absorption to localized carriers. That is, the slow relaxation of the induced absorption in a-As$_2$S$_3$ requires a slow recombination rate in a-As$_2$S$_3$ which in turn sets an upper limit of 10^{-2} cm^2 V^{-1} sec^{-1} on the mobility of the absorbing carriers in a-As$_2$S$_3$ during the first 300 psec. Such a low mobility implies well-localized carriers.[13] We obtain this limit using Langevin's

formula[14]

$$\gamma = (4\pi e/\epsilon)(\mu_e + \mu_h)N , \qquad (5)$$

where e is the electronic charge, ϵ the static dielectric constant, and μ_e and μ_h the electron and hole mobilities, respectively. (We use the absence of detectable relaxation during the 300-psec observation period to set an upper limit on the recombination rate of 3×10^8 sec^{-1}.) The more rapid relaxation of the induced absorption in c-As_2S_3 is in agreement with the larger mobility of the carriers in the crystalline host. That is, the carrier mobilities are of order unity[5] in c-As_2S_3 which, with use of $N = 10^{17}$ cm^{-3} and Langevin's formula, gives the observed relaxation rate of 7×10^{10} sec^{-1} within experimental error.

The spectral and temporal properties of excited As_2S_3 thus combine to support strongly an assignment of this transient absorption to localized carriers. The observed relaxation rates are also consistent with the recombination behavior expected on the basis of earlier mobility measurements of localized carriers.[4,5] The resulting upper limit of 1 psec implied for carrier localization time places significant constraints on models proposed to explain localized states in As_2S_3. For example, if the localization is attributed to trapping at defects[15] then Langevin's equation sets a lower limit on the product of the mobility of the excited carriers during the first 1 psec, μ, and the density of charged traps, N_t, of $\mu N_t \geqslant 5 \times 10^{18}$ cm^{-1} V^{-1} sec^{-1}. This requires either a large hot-carrier mobility or a high density of traps, or both. If the localization is attributed instead to polaron formation, then it is necessary to postulate a virtual absence of any energy barrier to polaron formation.[16] Finally, whatever model is used, some mechanism is required to explain the difference between the spectra of the transient and metastable absorptions shown in Fig. 3 and the difference which they imply in the distribution of occupied trapping sites in those two cases.

Thanks are due D. Emin, J. P. Gordon, G. Beni, D. Adler, M. Kastner, G. Pfister, F. Schmidlin, and P. A. Wolff for discussions and F. A. Beisser, P. M. Bridenbaugh, and D. H. Olsen for able technical assistance. One of us (A.M.) acknowledges receipt of a grant from the European Space Agency.

[1]S. G. Bishop, U. Strom, and P. C. Taylor, Phys. Rev. B 15, 2278 (1977).

[2]The contrasting dynamics of delocalized electronic states obtained with similar time resolution are described in C. V. Shank, R. L. Fork, R. F. Leheny, and J. Shah, Phys. Rev. Lett. 42, 112 (1979).

[3]Transient induced absorption in chalcogenide glasses has recently been observed by others, but without the short time resolution obtained here. See, e.g., M. Kastner and J. Orenstein, in Physics of Semiconductors —1978, edited by B. L. H. Wilson, The Institute of Physics Conference Series No. 43 (The Institute of Physics, Bristol and London, 1979), p. 1301. Professor Kastner also recently informed us of evidence for a time-dependent mobility and hence a time-dependent distribution of occupied trapping sites.

[4]S. W. Ing, Jr., J. H. Neyhart, and F. Schmidlin, J. Appl. Phys. 42, 696 (1971). These authors find the carrier mobility too small to measure in a-As_2S_3, but do find evidence for a time-dependent evolution in the distribution of occupied trapping sites. For recent results, see G. Pfister and H. Scher, Adv. Phys. 27, 747 (1978).

[5]R. Zallen and D. F. Blossey, in Optical and Electrical Properties of Materials with Layered Structures, edited by P. A. Lee (Reidel, Dordrecht, 1976), p. 231.

[6]E. P. Ippen and C. V. Shank, Topics Appl. Phys. 18, 44 (1977).

[7]E. P. Ippen and C. V. Shank, in Proceedings of the First International Conference on Picosecond Phenomena, 1978, edited by C. V. Shank, E. P. Ippen, and S. L. Shapiro (Springer, New York, 1978), p. 103.

[8]The duration of pump and probe pulses was 0.5 psec; however, the band-edge disperison caused a difference of 1 psec in pump and probe delays in our 0.5-mm-thick samples for the wavelengths used for Fig. 1. We therefore take 1 psec as the lower limit on our resolution time.

[9]The pump experienced 24% linear absorption in our samples; however, that linear absorption was not effective in generating absorbing centers consistent with earlier work (see, e.g., Bishop, Strom, and Taylor, Ref. 1).

[10]We obtain this value for σ by using an upper limit of 1 on η to set a lower limit on σ of 0.3×10^{-16} cm^2 and an upper limit of 1 on the oscillator strength to set an upper limit on σ of 3×10^{-16} cm^2 (see Bishop, Strom, and Taylor, Ref. 1); we assume here a nominal bandwidth of ~ 2 eV). Our experimental uncertainty was due to errors in measuring spot size and beam power and did not exceed 3×. Bishop, Strom, and Taylor quote an uncertainty of 10× for their values of σ and N.

[11]We use the term trap in a generic sense to mean both traps due to defects and traps due to defects and traps due to self-trapping as by polaron formation.

[12]Transient photoluminescence consistent with a time-dependent evolution of the distribution of occupied trapping sites has been reported by M. A. Bosch and Jagdeep Shah, Phys. Rev. Lett. 42, 118 (1979).

[13]See, e.g., M. H. Cohen, J. Non-Cryst. Solids 4, 391 (1970).

[14]See, e.g., R. G. Kepler, in *Treatise on Solid State Chemistry*, edited by N. B. Hannay (Plenum, New York, 1976), Vol. 3, p. 650.

[15]N. F. Mott, E. A. Davis, and R. A. Street, Philos. Mag. **32**, 961 (1975).

[16]D. Emin, private communication. See also, R. C. Hughes and D. Emin, in *Proceedings of the First Topical Conference on the Physics of SiO_2 and Its Interfaces, Yorktown Heights, New York, 1978*, edited by S. T. Pantelides (Pergamon, New York, 1978).

Resolved Structure within the Broad-Band Vibrational Raman Line of Liquid H_2O from Polarization Coherent Anti-Stokes Raman Spectroscopy

N. I. Koroteev,[a] M. Endemann, and R. L. Byer

Applied Physics Department, Stanford University, Stanford, California 94305

(Received 21 May 1979)

We have resolved individual components of the broad vibrational band of liquid water by using polarization coherent anti-Stokes (active) Raman spectroscopy. None of the existing models of liquid water based on the unresolved spontaneous Raman spectrum describe in full the observed spectra.

The unambiguous resolution of close and overlapping lines is one of the most important and difficult problems in spectroscopy. In spontaneous Raman spectroscopy of condensed substances the solution to this problem is a curve-fitting procedure involving a formal resolution of observed bands into a number of symmetrical lines of chosen shape and intensity. However, this technique suffers from the lack of uniqueness as a consequence of the lack of resolution. A well-known and important example of the lack of uniqueness is the variety of models proposed to describe the spontaneous Raman line shape of liquid water in the $3200-3600-cm^{-1}$ stretching-vibrational region.[1-5]

In this Letter we show that active control of the polarization in coherent anti-Stokes (active) Raman spectroscopy (CARS) offers the spectroscopist a new tool with which to probe the inner structure of broad Raman bands. We apply the technique to the $3400-cm^{-1}$ band of liquid water and resolve spectral details that can be used to verify existing models of this band and thus the structure of water in the liquid state.

The ability of polarization CARS to resolve components was discussed and experimentally used to resolve the doublet structure of the $1305-cm^{-1}$ Raman line of an aqueous solution of HNO_3.[6,7] Here we develop this technique in more detail with emphasis on broad featureless bands.

Consider a simple example of a pair of closely spaced Raman lines with Lorentzian line shapes and identical linewidths and intensities but with slightly different depolarization ratios (i.e., $\rho_1 = 0.32$ and $\rho_2 = 0.35$). Figure 1(a) shows the resulting spontaneous Raman band shape when the two components are closer than their full width at half maximum (FWHM) linewidths. The band shape becomes indistinguishable from the individual components and hence the band is unresolved. A similar unresolved band shape occurs for ordinary CARS where the frequency dispersion of $|\chi_{1111}^{(3)}(\omega_a; \omega_1, -\omega_2)|^2$ is measured as shown in Fig. 1(b).

However, polarization CARS does allow the band shape to be resolved as shown in Fig. 1(c). Here the polarization vectors $\vec{e}_1$ and $\vec{e}_2$ of the linearly polarized waves at frequencies ω_1 and ω_2 make an angle $\rho = 70°$ with respect to each
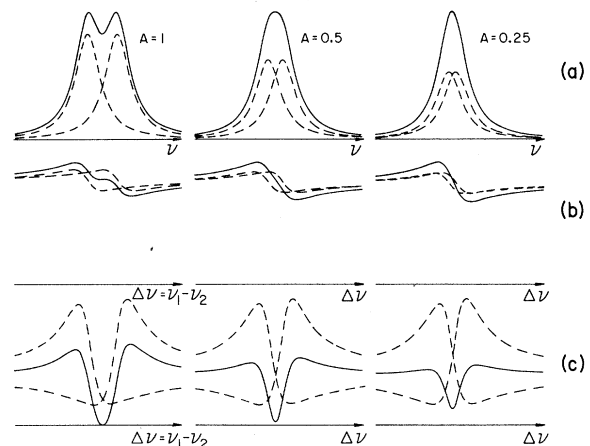

FIG. 1. Pair of overlapping lines in (a) spontaneous Raman spectroscopy, (b) ordinary CARS, and (c) polarization CARS. The parameter of curves is the relative distance between the line centers, $A = (\Omega_1 - \Omega_2)/$ FWHM. In (c), the angle ϵ between $\vec{p}_{NR}$ and the normal of the analyzer transmission plane is chosen to be $\epsilon = 0.14°$; $\chi_{1111}^{(3)R1}/\chi_{1111}^{(3)NR} = 0.1$.